Coexistence and Competition of the Short-Range Incommensurate Antiferromagnetic Order with the Superconducting State of BaFe_{2-x}Ni_{x}As_{2}

Huiqian Luo, Rui Zhang, Mark Laver, Zahra Yamani, Meng Wang, Xingye Lu, Miaoyin Wang, Yanchao Chen, Shiliang Li, Sung Chang, Jeffrey W. Lynn, and Pengcheng Dai

Phys. Rev. Lett. **108**, 247002 — Published 12 June 2012

DOI: 10.1103/PhysRevLett.108.247002

Coexistence and competition of the short-range incommensurate antiferromagnetic order with superconductivity in $BaFe_{2-x}Ni_xAs_2$

Huiqian Luo,[1] Rui Zhang,[1] Mark Laver,[2,3] Zahra Yamani,[4] Meng Wang,[1] Xingye Lu,[1,5] Miaoyin Wang,[5] Yanchao Chen,[1,6] Shiliang Li,[1] Sung Chang,[7] Jeffrey W. Lynn,[7] and Pengcheng Dai[5,1,*]

[1]*Beijing National Laboratory for Condensed Matter Physics, Institute of Physics, Chinese Academy of Sciences, Beijing 100190, China*
[2]*Laboratory for Neutron Scattering, Paul Scherrer Institute, CH-5232 Villigen, Switzerland*
[3] *Department of Physics, Technical University of Denmark, DK-2800 Kgs. Lyngby, Denmark*
[4]*Canadian Neutron Beam Centre, National Research Council, Chalk River Laboratories, Chalk River, Ontario K0J 1J0, Canada*
[5] *Department of Physics and Astronomy, The University of Tennessee, Knoxville, Tennessee 37996-1200, USA*
[6]*Science and Technology on Nuclear Data Laboratory, China Institute of Atomic Energy, Beijing 102413, China*
[7]*NIST Center for Neutron Research, National Institute of Standards and Technology, Gaithersburg, Maryland 20899, USA*

Superconductivity in the iron pnictides develops near antiferromagnetism, and the antiferromagnetic (AF) phase appears to overlap with the superconducting phase in some materials such as $BaFe_{2-x}T_xAs_2$ (where T = Co or Ni). Here we use neutron scattering to demonstrate that genuine long-range AF order and superconductivity do not coexist in $BaFe_{2-x}Ni_xAs_2$ near optimal superconductivity. In addition, we find a first-order-like AF to superconductivity phase transition with no evidence for a magnetic quantum critical point. Instead, the data reveal that incommensurate short-range AF order coexists and competes with superconductivity, where the AF spin correlation length is comparable to the superconducting coherence length.

High-temperature superconductivity (high-T_c) in iron pnictides arises at the border of antiferromagnetism [1–3]. Since magnetic excitations may be responsible for electron pairing and superconductivity [4–7], it is essential to understand the doping and temperature dependence of the antiferromagnetic (AF) spin correlations. For electron-doped iron pnictides such as $BaFe_{2-x}T_xAs_2$ (where T = Co or Ni), the Néel temperature (T_N) of the system decreases gradually with increasing electron-doping level x and the AF phase appears to overlap with the superconducting phase [8–10]. This raises the question concerning the role of quantum criticality [11] and the coexisting AF order and superconductivity to the superconducting pairing mechanism [12, 13]. Here we use neutron scattering and transport measurements to show that genuine long-range AF order does not coexist with superconductivity in $BaFe_{2-x}Ni_xAs_2$ near optimal doping. With increasing x, the static AF order in $BaFe_{2-x}Ni_xAs_2$ changes abruptly from a commensurate wave vector for $x = 0.085$ to an incommensurate wave vector with short-range order for $x = 0.092, 0.096$. While the ordered moment decreases smoothly from $x = 0.085$ to 0.096, the Néel temperature (T_N) changes slowly from $\sim$47 K for $x = 0.085$ to $\sim$35 K for $x = 0.096$ before vanishing at $x = 0.1$. In addition, we find that the short-range incommensurate AF order directly competes with superconductivity, and there is no evidence for a conventional magnetic quantum phase transition between the two phases. Therefore, the presence of microscopic coexisting long-range AF and superconducting phases and a magnetic quantum critical point (QCP) between the AF and superconducting phase are not essential for superconductivity in the $BaFe_{2-x}T_xAs_2$ family of materials.

In earlier neutron and X-ray scattering work on $BaFe_{2-x}T_xAs_2$, the competition between coexisting superconductivity and antiferromagnetism was inferred from the reduction of the magnetic Bragg peak intensity below T_c [14–18]. If superconductivity and static long-range AF order coexist microscopically and compete for the same electrons, the superconducting pairing symmetry is most likely sign-reversed $s^{\pm}$-wave [12, 13]. However, muon spin rotation (μSR) experiments on underdoped $BaFe_{1.89}Co_{0.11}As_2$ suggest an incommensurate spin density wave below $T^{mag} \approx 32$ K with a reduced ordered magnetic moment below $T_c = 21.7$ K [19]. Neutron scattering reveals that the commensurate AF order at the wave vector $Q = (0.5, 0.5, 1)$ becomes transversely incommensurate at $Q = (0.5 - \delta, 0.5 + \delta, 1)$ (inset in Fig. 1a) for $BaFe_{2-x}Co_xAs_2$ with $0.112 < x < 0.12$ [20].

We carried out systematic neutron scattering experiments on $BaFe_{2-x}Ni_xAs_2$ using C-5, Rita-2, and BT-7 triple-axis spectrometers at the Canadian Neutron Beam Center, Paul Scherrer Institute, and NIST Center for Neutron Research (NCNR), respectively. For C-5 and BT-7 thermal triple-axis spectrometers, the final neutron energies were set to $E_f = 14.56$ and $E_f = 13.8$ meV, respectively, with pyrolytic graphite (PG) as monochromator, analyzer, and filters. For Rita-2 measurements, the final energy was $E_f = 4.6$ meV and a cooled Be filter was additionally used as a filter. High quality single crystals were grown by FeAs self-flux method as described previously [21]. We define the wave vector Q at (q_x, q_y, q_z) as $(H, K, L) = (q_x a/2\pi, q_y b/2\pi, q_z c/2\pi)$ reciprocal lattice units (rlu) using the tetragonal unit cell, where

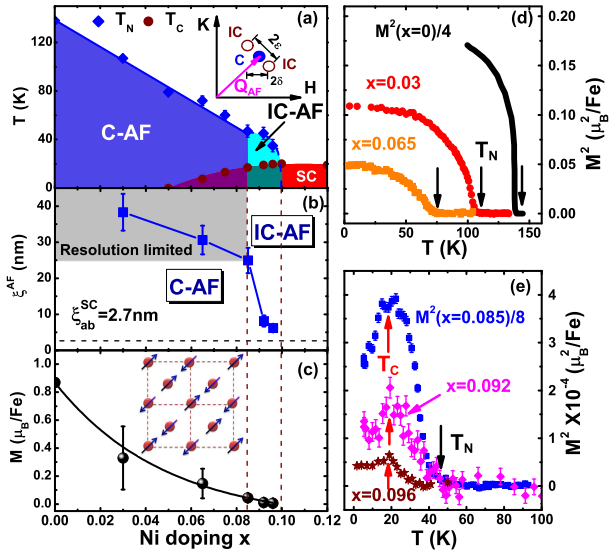

FIG. 1: (a) Electronic phase diagram of $BaFe_{2-x}Ni_xAs_2$ as a function of x. The long-range commensurate AF (C-AF) order changes into short range incommensurate AF (IC-AF) order for $x = 0.085 - 0.096$. The optimal superconductivity occurs at $x = 0.10$, where the static AF order is suppressed [22]. The inset shows positions of C-AF and IC-AF positions in reciprocal space in tetragonal notation, where $\delta = \epsilon/\sqrt{2}$. (b) The Ni-doping dependence of the in-plane AF spin-spin correlation length. For x=0.096, we have $\xi^{AF} \approx 66$ Å and the superconducting coherence length $\xi^{SC}_{ab} \approx 27$ Å [40]. (c) The doping dependence of the ordered magnetic moment M [23]. (d) Temperature dependence of the magnetic order parameter at $Q = (0.5, 0.5, 1)$ and (0.5, 0.5, 3) AF Bragg positions for $x = 0, 0.03, 0.065$, and (e) $x = 0.085, 0.092, 0.096$.

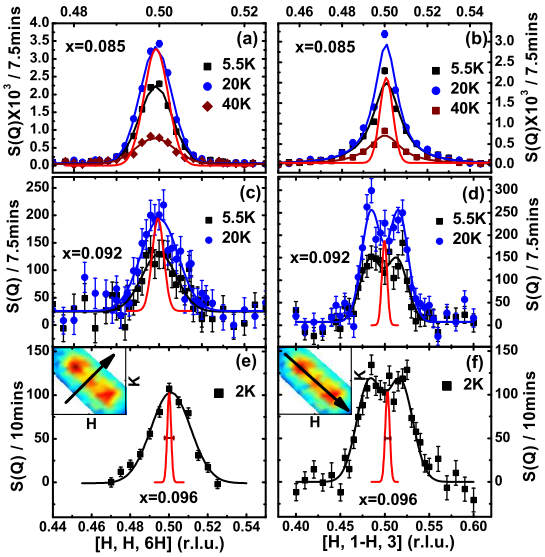

FIG. 2: Temperature and wave vector dependence of the C-AF and IC-AF scattering for $BaFe_{2-x}Ni_xAs_2$ with $x = 0.085, 0.092$ and 0.096. Samples are aligned in the $[H, H, 6H]$ and $[H, 1-H, 3]$ scattering plane. The solid red lines are the instrumental resolutions obtained using $\lambda/2$ scattering from the $(1, 1, 6)$ nuclear Bragg peak above T_N without filter. Data in (a-d) are collected on C-5. (a,b) Longitudinal and transverse scans at different temperatures through the $(0.5, 0.5, 3)$ AF Bragg peak for $x = 0.085$. The scattering is commensurate in both directions but not instrumental resolution limited. The solid lines in transverse scans are Lorentzian fits to the data. (c,d) Identical scans using the same experimental setup for $x = 0.092$, which show clear incommensurate scattering along the transverse direction. (e,f) Longitudinal and transverse scans for $x = 0.096$ at $Q = (0.5, 0.5, 3)$ collected on Rita-2. The solid horizontal bars are the calculated instrumental resolution, determined by the supermirror guide before the monochromator, the 80′ collimation, the radial collimator of the Be filter (about 150′), the neutron absorbing guide after the analyzer (effective collimation of 40′) and a sample mosaic spread of ∼15′. Inserts show the color images of incommensurate peaks centered around $Q = (0.5, 0.5, 3)$ and the scan directions at 2 K.

$a \approx b \approx 3.96$ Å, and $c = 12.77$ Å.

Figure 1a shows the electronic phase diagram of $BaFe_{2-x}Ni_xAs_2$ as a function of Ni-doping x as determined from our neutron scattering experiments, where the commensurate to incommensurate AF phase transition occurs between $x = 0.085$ and 0.092. Figures 1b, 1c, 1d and 1e show the Ni-doping dependence of the spin correlation length, moment, and magnetic order parameters, respectively. While the Néel temperatures decrease gradually with increasing x for $0 \leq x \leq 0.065$ as shown in Fig. 1d [14–18], they decrease rather slowly for $x = 0.085, 0.092, 0.096$ before vanishing abruptly at $x = 0.1$ (Figs. 1a and 1e) [22]. For comparison, the ordered moment decreases smoothly to zero with increasing x at 0.1 (Fig. 1c), consistent with the presence of a magnetic QCP [11]. However, the static spin correlation length, which is instrumental resolution limited for $x < 0.085$, decreases abruptly for samples with incommensurate AF order (Fig. 1b) [23]. This is contrary to the magnetic QCP in $CeFeAs_{1-x}P_xO$ where the commensurate AF order is resolution limited at all x as the ordered moment vanishes with $x \to 0.4$ [24].

To demonstrate the doping evolution of the AF order through the commensurate to incommensurate AF phase transition, we summarize in Fig. 2 longitudinal and transverse scans along the $[H, H, 6H]$ and $[H, 1-H, 3]$ directions for $x = 0.085, 0.092$, and 0.096 at different temperatures, where the solid red lines indicate the instrumental resolution. For $x = 0.085$, the scattering is commensurate along both the longitudinal and transverse directions, but not instrumental resolution limited (Figs. 2a and 2b). Furthermore, the lineshape of transverse scan is not a Gaussian but can be fit with a Lorentzian. Figures 2c and 2d show identical scans using the same instrument for the $x = 0.092$ sample. Here, we find broad commensurate scattering in the longitudinal direction and clear incommensurate peaks in the transverse direction. Figures 2e and 2f plot longitudinal and trans-

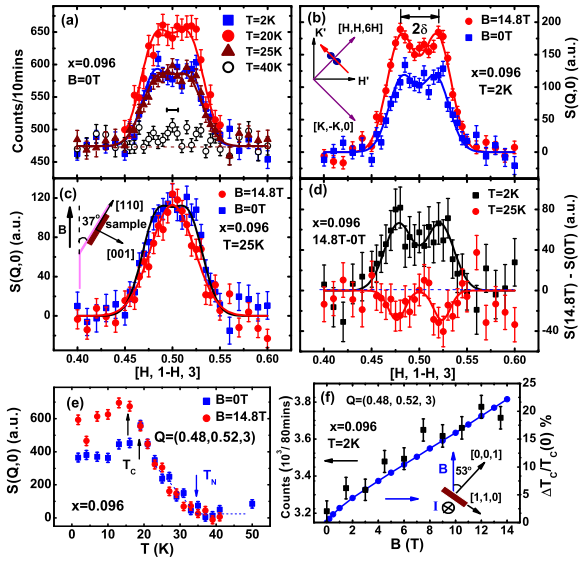

FIG. 3: Effect of a 14.8 T magnetic field on the short-range incommensurate AF order in the $x = 0.096$ sample. For this experiment on Rita-2, a single crystal of mass about 0.5 gram and mosaic of 0.45° was aligned in a 15-T magnet in the $[H, H, 6H]$ and $[H, 1-H, 3]$ scattering plane as shown in the inserts of (b) and (c). Neutrons of $E_i = E_f = 4.6$ meV were selected, with the nine blades of the analyzer set to probe different points in reciprocal space. Two filters were employed to remove higher order neutrons: a pyrolytic graphite placed just before the sample, along with a $80'$ collimator, and cooled Be placed just after the sample. (a) Transverse scans at zero field and at $T = 2$ K (below T_c), 20 K (around T_c) , 25 K ($T_c < T < T_N$) and 40 K (above T_N). The incommensurability $\pm\delta$ remains at 0.018 for all measured temperatures. (b) Comparison between zero and 14.8 T fields at $T = 2$ K. The 14.8 T magnetic field clearly enhances the IC-AF order. (c) Identical scans at $T = 25$ K, where a 14.8 T field suppresses the incommensurate AF order. (d) The effect of a 14.8 T field on the incommensurate AF order. While the field enhances the IC-AF order at 2 K, it may suppress the IC-AF order in the normal state. (e) Temperature dependence of the magnetic order parameters at the incommensurate position $Q = (0.48, 0.52, 3)$ for 0 and 14.8 T fields. The superconducting transition temperature T_c is seen to shift from ∼19 K to ∼15 K. (f) Magnetic field dependence of the AF Bragg peak intensity at $Q = (0.48, 0.52, 3)$. The data show a linear field dependence, consistent with a field-induced suppression of superconducting transition temperature $\Delta T_c = (T_c(0) - T_c(B))/T_c(0)$ as determined from resistivity measurements on the same sample (solid blue circles and lines).

verse scans along the aforementioned directions for the $x = 0.096$ sample. Converting these widths into real space [23], we find that the static spin correlation length along the longitudinal direction is only 62 ± 5 Å while it is 81 ± 15 Å and 249 ± 35 Å for the $x = 0.092$ and 0.085 samples, respectively.

Figure 3a-3c shows the detailed temperature dependence of the transverse scans at zero and a field of 14.8 T. At zero field, transverse scans are featureless at $T = 40$ K ($> T_N$) but show broad peaks indicative of incommensurate AF short-range order below $T_N \approx 35$ K. At $T = 20$ K just above T_c, the peak intensity continues to increase, but decreases upon further cooling to 2 K (Fig. 3a). These results are consistent with earlier work on $BaFe_{2-x}Co_xAs_2$ [20]. Upon applying a 14.8 T field aligned at ∼37° out of the FeAs-plane (Fig. 3b), we see that the broad peak at zero field and 2 K increases in intensity and becomes two clear incommensurate peaks centered at $Q = (0.5-\delta, 0.5+\delta, 3)$ with $\delta = 0.018 \pm 0.002$ rlu. For a temperature just above T_c at 25 K, the broad peaks appear to merge into a single commensurate peak centered at $Q = (0.5, 0.5, 3)$ (Fig. 3c). To determine the net effect of a 14.8 T field, we show in Fig 3d the field-on minus field-off difference plots. At $T = 2$ K, the effect of a field is to induce clear incommensurate peaks, different from the field effect on superconducting $BaFe_{2-x}Ni_xAs_2$ with lower x [18]. At a temperature ($T = 25$ K) just above T_c, the effect of a field appears to be opposite and suppresses the incommensurate AF order. Figure 3e shows the temperature dependence of the scattering at the incommensurate position at zero and 14.8 T. At zero field, the data reveal a clear suppression of the magnetic intensity at T_c. A 14.8 T field reduces T_c from 19 K to 15 K and enhances the incommensurate AF order. The intensity of the incommensurate AF scattering increases linearly with increasing field, consistent with the field-induced reduction in the superconducting transition temperature as determined from resistivity measurements (Fig. 3f). However, the linewidths of the incommensurate peaks remain unchanged at 2 K (Fig. 3b). Therefore, superconductivity competes with the short-range incommensurate AF order instead of the long-range AF order.

In transport and nuclear magnetic resonance (NMR) experiments on isoelectronic $BaFe_2(As_{1-x}P_x)_2$ [25–28], a magnetic QCP has been identified at $x = 0.33$, which is believed to play an important role in the superconductivity of these materials [11]. For $BaFe_{2-x}Co_xAs_2$, recent systematic ultrasonic measurements [29] suggest the presence of a structural QCP near optimal superconductivity, where the structural distortion associated with the static AF order vanishes. These results are consistent with NMR measurements, where the strength of the paramagnetic spin fluctuations diverges for Co concentration near optimal superconductivity [30]. If Ni-doping in $BaFe_2As_2$ is equivalent to twice the Co-doping [31], one should also expect a structural and magnetic QCP near optimal superconductivity for $BaFe_{2-x}Ni_xAs_2$. Since the incommensurate AF spin correlations for the $x = 0.092, 0.096$ samples clearly do not increase with decreasing temperature, it is difficult to reconcile this result with a magnetic QCP, where one expects a diverging spin-spin correlation length as $T \to 0$ K. Furthermore, the Néel temperature of $BaFe_{2-x}Ni_xAs_2$ suddenly

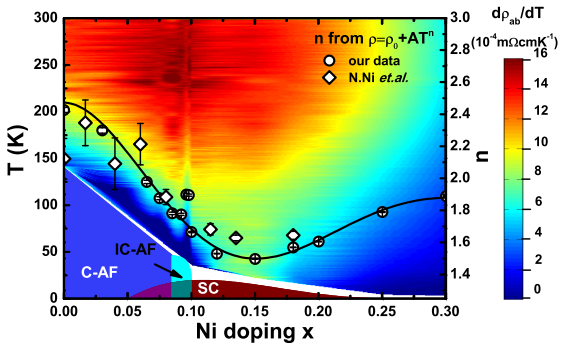

FIG. 4: Temperature and doping dependence of in-plane resistivity of $BaFe_{2-x}Ni_xAs_2$ in the normal state ($T > T_N, T > T_c$) derived from ref. [21] and ref. [33], where $\rho_{ab}(T = 300\ \mathrm{K})$ is assumed to decrease linearly with increasing x. The gradient color is the first order differential of resistivity in the normal state, $d\rho_{ab}/dT$, suggesting the linear term emerges from the overdoped regime. Open symbols are the exponent n deduced from fitting $\rho = \rho_0 + AT^n$ in the normal state, which minimizes to $n \approx 1.5$ near $x = 0.15$. An anomalous n is found for the IC-AF sample.

vanishes at $x = 0.1$ from $T_N \sim 35$ K for $x = 0.096$. Therefore, instead of a magnetic QCP, the incommensurate AF order to superconductivity phase transition in $BaFe_{2-x}Ni_xAs_2$ appears to be a first order, much like that of the $LaFeAsO_{1-x}F_x$ family of materials [32].

If there is a magnetic QCP in the phase diagram of $BaFe_{2-x}Ni_xAs_2$ near $x = 0.10$ where the static long-range AF order vanishes [22], the temperature dependence of the resistivity $\rho = \rho_0 + AT^n$ should have an exponent $n \approx 1$ near $x = 0.1$ within a single band model similar to that of $BaFe_2(As_{1-x}P_x)_2$ at $x = 0.33$ [28]. Figure 4 shows the electron-doping dependence of the resistivity exponent n obtained by fitting the temperature dependence of the resistivity of $BaFe_{2-x}Ni_xAs_2$ [21, 33]. The resistivity exponents show a broad minimum with $n \approx 1.5$ near $x = 0.15$. Similar analysis on the in-plane resistivity data of $BaFe_{2-x}Co_xAs_2$ in the normal state also yielded minimum n in the overdoped region, clearly different from that for $BaFe_2(As_{1-x}P_x)_2$ [28]. Therefore, our data suggest no magnetic QCP near the boundary of AF and superconducting phases in $BaFe_{2-x}T_xAs_2$. This is consistent with the more accurate two band analysis of the normal state resistivity for $BaFe_{2-x}T_xAs_2$ [34, 35], where a Fermi liquid like coefficient $n = 2$ was found for optimally doped $BaFe_{2-x}T_xAs_2$ again suggesting no QCP near optimal superconductivity.

The observation of competing static short-range incommensurate AF order with superconductivity and the first-order-like AF to superconductivity phase transition raises the question concerning how AF order microscopically coexists with superconductivity in Fe-based superconductors [18]. In a recent ^{57}Fe Mössbauer spectroscopy study of $BaFe_{2-x}Ni_xAs_2$, a small reduction in magnetic hyperfine field below T_c was found for the $x = 0.085$ sample [36]. Although such measurements suggest coexisting AF order and superconductivity on a length scale of ∼27 Å [36], Mössbauer spectroscopy cannot provide a precise length scale of the AF spin correlations and their doping dependence. For comparsion, our data show that AF order at this doping level is commensurate with a correlation length of ∼250 Å (Figs. 1b and 2a). For hole-doped $Ba_{1-x}K_xFe_2As_2$, μSR [37] and neutron powder diffraction [38, 39] measurements have suggested microscopic coexisting AF and superconducting phases in the underdoped regime. However, these measurements did not probe the region of the phase diagram close to optimal superconductivity, and were unable to provide a length scale for the AF order that coexists with the superconductivity. From Figs. 1-3, we see that the static incommensurate AF order competing with superconductivity has a spin-spin correlation length of ∼60 Å. This means that the incommensurate AF order has a similar length scale to the superconducting coherence length (∼27 Å) [40], and that, near optimal doping, there is no long-range AF order coexisting with superconductivity. Instead, our data can be understood in two scenarios: first, the two orders coexist microscopically and homogeneously, and compete for the same itinerant electrons [12, 13], such that superconductivity occurs at the expense of the static AF order. When a magnetic field is applied, the superconducting gap $\Delta(B)$ and T_c decrease with increasing field via $\Delta(B)/\Delta(0) = T_c(B)/T_c(0) = \sqrt{1 - B/B_{c2}}$ [41]. In the low-field limit, we have $B/B_{c2} \propto \Delta T_c/T_c(0)$. Therefore, the field-induced AF order should be proportional to the field-induced reduction in T_c, consistent with the data in Fig. 3f. Alternatively, the competition is mesoscopic: phase-separation occurs with superconducting and non-superconducting, AF-ordered nano-regions of length scale ∼60 Å. In this picture, the superconducting electrons do not directly contribute to the static AF order, and superconductivity only affects the AF order through a proximity effect. Here, one can imagine that the field-induced non-superconducting vortices have incommensurate AF order, much like field-induced AF vortices in some copper oxide superconductors [42]. This is also consistent with the first-order-like AF to superconductivity transition with increasing x. Since our neutron diffraction measurements of the bulk of the sample cannot resolve superconducting from non-superconducting parts of the sample, we find both scenarios are consistent with our observation of short-range AF order with superconductivity near optimal doping.

We thank Jiangping Hu, Qimiao Si, Daoxin Yao, Hai-Hu Wen, and Xingjiang Zhou for helpful discussions and transport measurements. The work at IOP, CAS, is supported by MOST (973 project: 2011CBA00110, 2010CB833102, and 2012CB821400) and NSFC (No.11004233). The work at UTK is supported by the U.S. NSF-DMR-1063866 and NSF-OISE-0968226. Part of the work is based on experiments per-

formed at the Swiss Spallation Neutron Source, Paul Scherrer Institute, Villigen, Switzerland. M. L. acknowledges support from DanScatt.

* Electronic address: pdai@utk.edu

[1] Y. Kamihara, T. Watanabe, M. Hirano, and H. Hosono, J. Am. Chem. Soc. **130**, 3296-3297 (2008).
[2] C. de la Cruz *et al.*, Nature (London) **453**,899 (2008).
[3] J. Zhao *et al.*, Nature Mater. **7**, 953 (2008).
[4] P. J. Hirschfeld, M. M. Korshunov, I. I. Mazin, Rep. Prog. Phys. **74**, 124508 (2011).
[5] A. V. Chubukov, Physica C **469**, 640 (2009).
[6] F. Wang and D.-H. Lee, Science **332**, 200 (2011).
[7] J. P. Hu and H. Ding, Scientific Reports **2**, 381 (2012).
[8] N. Ni *et al.*, Phys. Rev. B **78**, 214515 (2008).
[9] J.-H. Chu, J. G. Analytis, C. Kucharczyk, and I. R. Fisher, Phys. Rev. B **79**, 014506 (2009).
[10] C. Lester *et al.*, Phys. Rev. B **79**, 144523 (2009).
[11] E. Abrahams and Q. Si, J. Phys.: Condens. Matter **23**, 223201 (2011).
[12] R. M. Fernandes *et al.*, Phys. Rev. B **81**, 140501(R) (2010).
[13] R. M. Fernandes and J. Schmalian, Phys. Rev. B **82**, 014521 (2010).
[14] D. K. Pratt *et al.*, Phys. Rev. Lett. **103**, 087001 (2009).
[15] A. D. Christianson *et al.*, Phys. Rev. Lett. **103**, 087002 (2009).
[16] Miaoyin Wang *et al.*, Phys. Rev. B **81**, 174524 (2010).
[17] M. G. Kim *et al.*, Phys. Rev. B **82**, 180412(R) (2010).
[18] Miaoyin Wang *et al.*, Phys. Rev. B **83**, 094516 (2011).
[19] P. Marsik *et al.*, Phys. Rev. Lett. **105**, 057001 (2010).
[20] D. K. Pratt *et al.*, Phys. Rev. Lett. **106**, 257001 (2011).
[21] Yanchao Chen *et al.*, Supercond. Sci. Technol. **24**, 065004 (2011).
[22] S. Chi *et al.*, Phys. Rev. Lett. **102**, 107006 (2009).
[23] See supplementary material for information.
[24] C. de la Cruz *et al.*, Phys. Rev. Lett. **104**, 017204 (2010).
[25] S. Jiang *et al.*, J. Phys. Condens. Matt **21**, 382203 (2009).
[26] S. Kasahara *et al.*, Phys. Rev. B **81**, 184519 (2010).
[27] Y. Nakai *et al.*, Phys. Rev. B **81**, 020503 (2010).
[28] Y. Nakai *et al.*, Phys. Rev. Lett. **105**, 107003 (2010).
[29] M. Yoshizawa *et al.*, J. Phys. Soc. Jpn. **81**, 024604 (2012).
[30] F. L. Ning *et al.*, Phys. Rev. Lett. **104**. 037001 (2010).
[31] S. L. Bud'ko, N. Ni, and P. C. Canfield, Phys. Rev. B **79**, 220516(R) (2009).
[32] M. Luetkens *et al.*, Nature Materials **8**, 305 (2009).
[33] N. Ni *et al.*, Phys. Rev. B **82**, 024519 (2010).
[34] D. Wu *et al.*, Phys. Rev. B **81**, 100512 (2010).
[35] N. Barišić *et al.*, Phys. Rev. B **82**, 054518 (2010).
[36] J. Munevar *et al.*, arXiv: 1111.5853v1.
[37] E. Wiesenmayer *et al.*, Phys. Rev. Lett. **107**, 237001 (2011).
[38] H. Chen *et al.*, Europhys. Lett. **85**, 17006 (2009).
[39] S. Avci *et al.*, Phys. Rev. B **83**, 172503 (2011).
[40] A. Yamatomo *et al.*, App. Phys. Lett. **94**, 062511 (2009).
[41] J. Zhao *et al.*, Phys. Rev. B **81**, 180505(R) (2010).
[42] B. Lake *et al.*, Nature (London) **415**, 299 (2002).